Chern Number Spins of Mn Acceptor Magnets in GaAs

T. O. Strandberg, C. M. Canali, and A. H. MacDonald

Phys. Rev. Lett. **106**, 017202 — Published 5 January 2011

DOI: 10.1103/PhysRevLett.106.017202

Chern number spins of Mn acceptor magnets in GaAs

T.O. Strandberg[1], C.M. Canali[1], and A.H. MacDonald[2]
[1]*School of Computer Science, Physics and Mathematics, Linnæus University. Smålandsgatan 26 39233 Kalmar-Sweden. and*
[2]*Department of Physics, University of Texas at Austin, Austin, Texas 78712, USA*

We determine the effective total spin J of local moments formed from acceptor states bound to Mn ions in GaAs by evaluating their magnetic Chern numbers. When individual Mn atoms are close to the sample surface, the total spin changes from $J = 1$ to $J = 2$, due to quenching of the acceptor orbital moment. For Mn pairs in bulk, the total J depends on pair orientation in the GaAs lattice and on the separation between the Mn atoms. We point out that Berry curvature variation as a function of local moment orientation can profoundly influence the quantum spin dynamics of these magnetic entities.

State-of-the-art STM techniques have made it possible to substitute transition metal impurities for individual atoms in semiconductor crystals[1, 2]. When the impurity behaves as a dopant, high-resolution STM scanning capabilities can then provide detailed information on the nature of the bound donor or acceptor states[1–7]. Advances in spin-polarized STM techniques are now making it possible to address the quantum spin dynamics of individual coupled acceptor-impurity systems[8]. These centers represent a new class of magnetic entities which we refer to as *donor* or *acceptor magnets*. They have precisely reproducible properties that are intermediate in character between those of atomic local moments and nanomagnets, have promise for applications in spintronics and quantum information processing, and act as the building blocks of ferromagnetism in semiconductors[9, 10].

The interpretation of ongoing [7] and future STM experiments requires a theoretical understanding of the quantum-spin properties of acceptor and donor magnets. For the specific case of individual Mn impurities in bulk GaAs it is known that the ground-state (GS) total angular momentum of the Mn centers is $J = 1$. This value is the result of antiferromagnetic coupling between the localized $S = 5/2$ Mn spin and the spin ($s = 1/2$) and orbital moment ($l = 1$) of the acceptor hole. The $J = 1$ character of the GS angular momentum of the Mn embedded atom is supported by ESR and infrared spectroscopy experiments[11, 12], and it is presently being investigated by STM techniques[7]. In connection to these STM experiments, the following questions remain outstanding: (i) What happens to the total angular momentum J when the dopant is close to the symmetry breaking surface providing STM access? (ii) Is there an effective "giant spin" describing the low-energy magnetic properties of two or more nearby embedded Mn impurities in GaAs, and what is its value? (iii) Can we determine an effective spin Hamiltonian describing the quantum dynamics of acceptor magnets? The answers to these questions depend on a complex interplay between the kinetic exchange coupling Mn and acceptor spins, and the variation of the acceptor-level orbital spinor with Mn spin orientation, which is controlled by spin-orbit interactions (SOI) and the crystalline environment.

In this Letter we describe an approach which is similar to ones used to quantize the slow vibronic degrees of freedom in molecular systems[13]. It can be used to quantize magnetization dynamics in any theory in which the magnetization direction is initially treated as a classical parameter, for example spin-density-functional theory. It identifies the effective total spin J of the Mn acceptor magnet with a topological Chern number which is the average of a Berry curvature electronic functional over all possible directions of the Mn acceptor magnetic moment. The procedure yields the expected $J = 1$ value for Mn in bulk GaAs. However when a Mn atom is close to a symmetry-breaking surface, we find that $J = 2$ because the orbital contribution of the acceptor is quenched. Mn pairs close to a surface always have $J = 4$, due to strong localization of the acceptor wave-function. Surprisingly, for Mn pairs in bulk GaAs we find that the total spin can switch between $J = 4$, $J = 3$, and $J = 2$ depending on the orientation of the pair in the crystal and the distance between the two Mn atoms. Our theory allows us to extract a quantum spin Hamiltonian for the magnetic centers. The spectrum of these Hamiltonians is affected by Berry curvature variation as a function of magnetization orientation, which is especially strong whenever there is a weakly avoided level crossing at the Fermi energy.

We start by introducing a microscopic tight-binding model that captures the salient electronic properties of Mn impurities in GaAs[14–16]. The Hamiltonian reads

$$H = H_{\rm band} + H_{\rm SO} + J_{pd} \sum_m \sum_{n[m]} \vec{s}_n \cdot \vec{S}_m \qquad (1)$$

where $H_{\rm band}$ contains the Slater-Koster parameters that reproduce the band structure of bulk GaAs plus parameters that account for the $4s$ and $4p$ orbitals of each substitutional Mn atom; the second term is a one-body atomic spin-orbit term. The third term describes an effective antiferromagnetic exchange interaction between a Mn spin $\vec{S}_m$ and its nearest-neighbor As p-spins $\vec{s}_n$. This is a kinetic pd exchange originating from the hybridization of the Mn 3d-levels with the As p-levels. We also include a spin-independent Coulomb potential associated with the

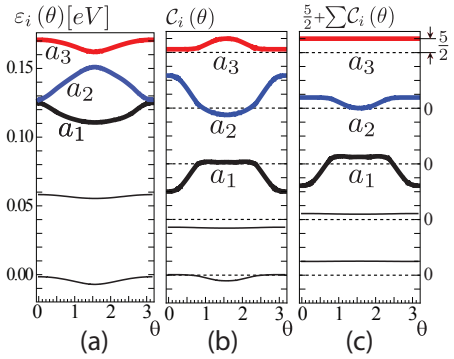

FIG. 1: (Color online) Electronic structure and Berry curvature for one Mn impurity in bulk GaAs as a function of the polar angle θ specifying the Mn magnetic moment direction relative to a cubic crystal axis. The coordinate system used for these plots has $\theta = 0$ parallel to the [001] axis, $(\theta = \pi/2, \phi = 0)$ parallel to [100], and $(\theta = \pi/2, \phi = \pi/2)$ parallel to [010] (see Fig. 2). (a) The three acceptor energy levels a_1, a_2, a_3 above the valence band edge. The topmost level a_3 (red curve) is the only one occupied by a hole; a_2 (blue curve) is the highest energy occupied orbital. (b) Berry curvatures for the individual levels in (a). The dashed lines mark the zero for a given curvature plot. (c) Cumulative level curvature plus the constant contribution 5/2 from the Mn impurity. The scale for curvature plots is indicated on the right axis of panel (c). The blue curve, in which the a_3 contribution is not included, is the one that is relevant to the Mn acceptor magnet. Adding the curvature of the acceptor level a_3 to the total curvature gives a constant equal to $5/2$ (flat red curve).

Mn ion[14, 16, 17]; we do not explicitly include the Mn $3d$ orbitals, and $\vec{S}_m$ represents a *classical* vector of magnitude $5/2$.

The Coulomb potential and level repulsion due to hybridization with the Mn d-levels together push acceptor states whose spins are aligned with the Mn magnetic moments above the valence-band edge[14, 16, 17]. Each Mn impurity introduces three acceptor levels (p_x, p_y, p_z) which would be degenerate in the absence of SOI. SOI's not only lift the degeneracy, but can also lead to a dependence of energies and orbitals on the direction of the Mn magnetic moment. For a neutral Mn impurity only the top most of these three states is occupied by a hole. Fig. 1(a) shows that this electronic structure is reproduced by the model of Eq. 1 implemented numerically for one substitutional Mn impurity in the middle of a 1200-atom GaAs cluster with periodic boundary conditions[23]. For a pair of Mn atoms, the lowest energy state of the system is usually the one in which the two Mn magnetic moments are ferromagnetically aligned[15]. For this configuration, the two sets of acceptor states form bonding and antibonding molecular orbitals. The two topmost empty levels are then split by an energy that is related to effective Mn-Mn exchange interaction, and varies strongly with the pair orientation and the distance between the two Mn[2, 15, 16].

The starting point to derive an effective "total spin" Hamiltonian is an approximate imaginary-time quantum action for the coherent spin magnetization direction $\hat{n}$[18, 19]

$$S[\hat{n}] \equiv \int d\tau \left[\langle \Psi[\hat{n}] | \nabla_{\hat{n}} \Psi[\hat{n}] \rangle \cdot \frac{\partial \hat{n}}{\partial \tau} + E[\hat{n}] \right] . \quad (2)$$

In Eq. (2), $|\Psi[\hat{n}]\rangle$ is the many-particle ground-state wave function obtained by diagonalizing the Hamiltonian (1), and $E[\hat{n}]$ is the total energy obtained by summing over occupied single-particle states. Here $\hat{n}$ represents the orientation of the Mn spin vectors $\vec{S}_m$, which are assumed to be ferromagnetically aligned when the Mn ions are not isolated. The first term in (2) is a Berry phase term, which for a closed path γ on the unit sphere is given by $\mathcal{P} = i \oint_\gamma d\hat{n} \cdot \langle \Psi | \nabla_{\hat{n}} \Psi \rangle$. The line integral can be converted into an integral over enclosed area with a gauge-invariant integrand known as the Berry curvature[20, 21],

$$\vec{\mathcal{C}}[\hat{n}] = i \nabla_{\hat{n}} \times \langle \Psi | \nabla_{\hat{n}} \Psi \rangle . \quad (3)$$

In our model, $\vec{\mathcal{C}}[\hat{n}] = \sum_i^{\rm occ} \vec{\mathcal{C}}_i[\hat{n}]$, the sum of the Berry curvatures $\vec{\mathcal{C}}_i[\hat{n}]$ of all occupied single-particle levels $i = 1, 2, \ldots, {\rm occ}$. In the absence of SOI, all $\mathcal{C}_i = \vec{\mathcal{C}}_i[\hat{n}] \cdot \hat{n}$ are constant and equal to the spin projection of each level, $\pm 1/2$. In this case $\vec{\mathcal{C}} \cdot \hat{n} = \sum_i^{\rm occ} \pm \frac{1}{2} = S$, where S is the total spin of the system. The effect of SOI is twofold. First, there is now an orbital contribution to the curvature. Second, $\vec{\mathcal{C}}_i[\hat{n}]$ varies with $\hat{n}$, as shown in Fig. 1(b).

The average of the Berry curvature over the unit sphere S^2 of all possible directions,

$$J = \tfrac{1}{4\pi} \int_{S^2} \vec{\mathcal{C}}[\hat{n}] \cdot \hat{n} \; dA \; , \quad (4)$$

is a topological invariant, known as first Chern number[22]. Although $\vec{\mathcal{C}}[\hat{n}]$ can fluctuate strongly, J is always a multiple of one-half[22]; its value can change only if the system suffers a level crossing at the Fermi level[18, 19]. It is useful to introduce single-level Chern numbers $j_i = \frac{1}{4\pi} \int_{S^2} \vec{\mathcal{C}}_i[\hat{n}] \cdot \hat{n} \; dA$, so that $J = \sum_i^{\rm occ} j_i$. When SOI's are included j_i can be different from $\pm 1/2$. The contribution from the spin-polarized Mn d-orbitals that are not explicitly included in our calculation are accounted for by adding $5/2$ to the total Berry curvature for each Mn ion in the system. As we explain below, the total Chern number J plays the role of the effective quantum spin of the Mn acceptor magnet.

We first discuss the case of one Mn impurity in GaAs and confirm that our approach yields sensible results. Indeed, as shown in Fig. 2(a), when the Mn is located in the bulk, solving our model numerically for a 1200-atom cluster gives $J = 1$, as expected. To understand this result, we observe that the total Chern number for a full valence band vanishes. The total Chern number of the acceptor magnet is therefore $J = 5/2 - j$, where j is the Chern number

Mn atoms	J	j
bulk	1	3/2
(sub)surface	2	1/2

(a) - Table I

Mn pairs - bulk	J	j_1	j_2
$\langle 110\rangle_{d=0.7a,\ 1.4a,\ 2.1a}$	4	1/2	1/2
$\langle 100\rangle_{d=a}$	3	1/2	3/2
$\langle 100\rangle_{d=2a,\ 3a}$	4	-1/2	3/2
$\langle 211\rangle_{d=1.2a}$	4	1/2	1/2
$\langle 211\rangle_{d=2a,\ 3a}$	3	3/2	1/2
$\langle 111\rangle_{d=1.7a}$	3	3/2	1/2
Mn pairs -(sub)surface	4	1/2	1/2

(b) - Table II

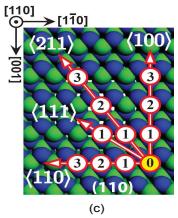

(c)

FIG. 2: (Color online) Calculated Chern numbers for Mn impurities in bulk GaAs or in the (110) surface and nearby sub-surfaces. (a) Results for one Mn impurity. J is the total Chern number and j the Chern number of the acceptor level. (b) Results for various Mn pairs $\langle lmn\rangle_d$ separated by distance d in units of the lattice constant a. j_1 and j_2 are the two acceptor Chern numbers. (c) Orientation $\langle lmn\rangle$ and separation of different Mn pairs on the (110) surface of GaAs.

of the topmost acceptor state which is occupied by a hole. As shown in Fig. 2(a), we find $j = 3/2 = 1/2 + 1$. The orbital contribution to j, due to SOI, appears in our approach because the orbital content of the topmost acceptor state varies with moment orientation. The orbital moment is locked to the spin-moment by strong SOI's. The result is different however, when the Mn impurity is located on the (110) surface[24], a case frequently considered in STM experiments. For this case we find that the orbital content of the acceptor wavefunction does not vary substantially with magnetization direction. The Chern number of the acceptor level only has a $j = 1/2$ spin contribution so that $J = 5/2 - 1/2 = 2$. Evidently symmetry breaking on the (110) surface, with only three nearest-neighbor As atoms instead of four, creates a local environment for a Mn whose symmetry is lower than the tetragonal symmetry seen by the impurity in bulk GaAs. As a result the acceptor orbital moment is completely quenched. (A direct calculation shows that $\langle a_3|\vec{L}|a_3\rangle = 0$.) Interestingly, our calculations show that j remains equal to $1/2$ also when the Mn is located on one of the immediate sub-surfaces below the top (110) surface. We expect that j should eventually switch to the bulk value when the Mn is located deeply below the surface, but this does not happen for the film thicknesses in the present simulation. Recent STM experiments[7] indicate that the GS spin multiplet for one Mn splits near the surface due to strain. Although in Ref. 7 the multiplet was interpreted as a $J = 1$ state, $J = 2$ is not excluded due to possible quasi-degeneracies of the levels.

We can now investigate magnetic clusters with two Mn atoms, where the resulting total spin is less intuitive. Fig. 2(b) shows the Chern numbers for several ferromagnetic Mn pairs, whose orientation $\langle lmn\rangle$ in the crystal and Mn separation d is described in Fig. 2(c). When the pair is positioned on the (110) surface or in one of its nearby sub-layers, we find that the individual Chern numbers of the two empty acceptor states are always $j_1 = j_2 = 1/2$, yielding a total Chern number $J = 2 * 5/2 - 2 * 1/2 = 4$. The situation for a Mn pair in bulk GaAs is more complex. We can see that, while for several pairs (e.g. all the $\langle 110\rangle$ pairs) $J = 4$, like for the surface case, other pairs have $J = 3$, and ferromagnetically coupled remote spins should have $J = 2$. In this second case one of the individual acceptor Chern numbers, j_1 or j_2, is equal to $3/2$, and in the latter case both have Chern number $3/2$. Clearly the presence of a second Mn affects the orbital magnetic properties of the other, in a way that depends both on pair orientation and Mn separation. The outcome for the pair is not easily predictable. For example, while the $\langle 100\rangle$ pair switches from $J = 3$ at the shortest Mn separation $d = a$ to $J = 4$ at larger separations, the $\langle 211\rangle$ pair behaves exactly in the opposite way.

In the remaining part of the paper we will extract a quantum spin Hamiltonian describing the dynamics associated with the moment orientation of acceptor magnets. We return to the action given by Eq. 2 and perform a change of variables[18, 19] from $\hat{n}(\theta,\phi)$ to $\hat{n}'(\theta',\phi')$ that transforms the Berry curvature $\mathcal{C}[\hat{n}]$ to a constant $\mathcal{C}'[\hat{n'}] = J$. This change of variables rescales the local curvature metric such that $\mathcal{C}\,(\theta,\phi)\sin(\theta)d\theta d\phi = J\sin(\theta)d\theta' d\phi'$. The real-time action for a path becomes

$$\mathcal{S}^{(J)}_{\rm spin}[\hat{n'}] \equiv \int_0^t dt' \left[i\,\vec{A}_J \cdot \frac{d\hat{n}'}{dt'} - E\{\hat{n}[\hat{n}'\,(t')]\}\right], \quad (5)$$

where $\vec{A}_J = J\hat{\phi}'\,(1-\cos\theta')\,/\sin\theta'$. Eq. 5 is the quantum action for an effective "total spin" quantum number J[21]. The second term in the integrand is the semiclassical Hamiltonian of the system, which is given by

$$\tilde{E}(\hat{n}') = (E\{\hat{n}[\hat{n}']\} = \langle J,\hat{n}'|\tilde{\mathcal{H}}|J,\hat{n}'\rangle \quad (6)$$

where $\tilde{\mathcal{H}}$ is the quantum spin Hamiltonian and $|J,\hat{n}'\rangle$ is a spin-J coherent state parametrized by the unit vector $\hat{n}'(\theta',\phi')$. The function $\tilde{E}(\hat{n}')$ is is the anisotropy energy transformed so that it also captures Berry curvature variation. The quantum Hamiltonian $\tilde{\mathcal{H}}$ is constructed by first expanding $\tilde{E}(\hat{n}')$ in spherical harmonics $\tilde{E}(\hat{n}') = \sum_{\ell=0}^{2J}\sum_{m=-\ell}^{\ell}\gamma_\ell^m Y_\ell^m\,(\hat{n}')$. We then use a formula[19] which relates the spherical harmonics expansion coefficients γ_λ^μ to the matrix elements $\tilde{\mathcal{H}}^{(J)}_{mm'} = \langle J,m|\tilde{\mathcal{H}}|J,m'\rangle$ of the quantum spin Hamiltonian:

$$\tilde{\mathcal{H}}^{(J)}_{mm'} = (-1)^{m'-J}\sum_{\lambda=0}^{2J}\sum_{\mu=-\lambda}^{\lambda}\gamma_\lambda^\mu\sqrt{\frac{2\lambda+1}{4\pi}} \times \begin{pmatrix} J & J & \lambda \\ m & -m' & \mu\end{pmatrix}\Big/\begin{pmatrix} J & J & \lambda \\ J & -J & 0\end{pmatrix} \quad (7)$$

where the quantities in parenthesis are Wigner 3J symbols. Once the Hamiltonian matrix has been obtained, it can be decomposed and rewritten as a combination of spin operators[19].

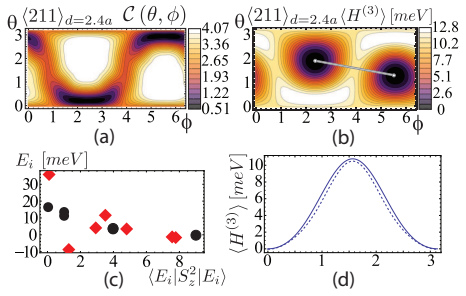

FIG. 3: (Color online) Effects of the Berry curvature on the quantum spin properties of the ferromagnetic Mn pair $\langle 211\rangle_{d=2.4a}$ in bulk GaAs. (a) Total Berry curvature landscape as a function of the pair magnetic moment direction. The two large dips at $\theta \approx 0, \pi$, relative to the [001] axis signal avoided crossings at the Fermi level. (b) Anisotropy energy landscape. (c) Spectrum of the effective quantum spin Hamiltonian with Chern number $J = 3$ *vs.* the expectation value of S_z^2. The black circles are the spectrum of $\mathcal{H}^3$ obtained by quantizing the classical magnetic anisotropy landscape. The red diamonds are the spectrum of $\tilde{\mathcal{H}}^3$, which includes Berry curvature effects. (d) Magnetic anisotropy barrier separating the two energy minima, plotted along the straight line in (b). The solid and dashed curves are for the cases when Berry curvature effects are excluded or included respectively.

As an example of this procedure, we show in Fig. 3 results for the Mn pair $\langle 211\rangle_{d=1.4a}$ in bulk GaAs. In panel (a) we plot the Berry curvature functional $\mathcal{C}[\hat{n}] = \mathcal{C}(\theta, \phi)$. The calculated Chern number for this pair is $J = 3$. The large dips of $\mathcal{C}(\theta, \phi)$ below this value for $\theta \approx 0, \pi$ signal the occurrence of narrowly avoided level crossings at the Fermi level, for two time-reversed directions. The corresponding magnetic anisotropy landscape is plotted in (b). According to our theory, we expect that in this case Berry phase variations strongly influence the spectrum of the quantum spin Hamiltonian. This is indeed the case, as shown in Fig. 3(c), where we plot the spectrum $\{E_i\}_{i=1,\ldots,2J+1}$ of the Hamiltonian obtained when Berry phase corrections are either included ($\tilde{\mathcal{H}}^3$, red diamonds) or absent ($\mathcal{H}^3$, black circles), versus $\langle E_i|S_z^2|E_i\rangle$. ($S_z$ is the z-component of the effective spin.) The difference in the two spectra has implications for the magnetic anisotropy landscape. In Fig 3 (d) we plot $\langle J, \vec{n}|\mathcal{H}^3|J, \vec{n}\rangle$ and $\langle J, \vec{n}|\tilde{\mathcal{H}}^3|J, \vec{n}\rangle$ respectively, along the line that joins the two minima (see Fig 3 (b)). The thickness of the barrier that separate them is reduced (in this case by a few percent) by Berry phase corrections. The dips in the curvature at level crossings increase the quantum tunneling rates of the magnetization between the two minima.

In conclusion, we have identified the effective total spin of Mn impurities in GaAs as a topological Chern number that includes both the contribution of the Mn spins and the spin and orbital moments of the acceptor states. The effective spin is dependent on proximity to the surface and its quantum Hamiltonian is modified by Berry phase corrections.

This work was supported by the Welch Foundation, by the National Science Foundation under grant DMR-0606489, the Faculty of Natural Sciences at Linnaeus University, and by the Swedish Research Council under Grant No: 621-2007-5019.

[1] D. Kitchen, A. Richardella, and A. Yazdani, J. Supercond. **18**, 23 (2005).
[2] D. Kitchen *et al.*, Nature **442**, 436 (2006).
[3] A. M. Yakunin *et al.*, Phys. Rev. Lett. **92**, 216806 (2004).
[4] A. M. Yakunin *et al.*, Phys. Rev. Lett. **95**, 256402 (2005).
[5] F. Marczinowski *et al.*, Phys. Rev. Lett. **99**, 157202 (2007).
[6] J. K. Garleff *et al.*, Phys. Rev. B **78**, 075313 (2008).
[7] J. K. Garleff *et al.*, Phys. Rev. B **82**, 035303 (2010).
[8] R. Wiesendanger, Rev. Mod. Phys. **81**, 1459 (2009).
[9] T. Jungwirth *et al.*, Rev. Mod. Phys. **78**, 809 (2006).
[10] K. Sato *et al.*, Rev. Mod. Phys. **82**, 1633 (2010).
[11] J. Schneider *et al.*, Phys. Rev. Lett. **59**, 240 (1987).
[12] M. Linnarsson *et al.*, Phys. Rev. B **55**, 6938 (1997).
[13] A. Bohm *et al.*, *The geometric phase in quantum systems* (Springer, Berlin Heidelberg, 2003).
[14] T. O. Strandberg, C. M. Canali, and A. H. MacDonald, Phys. Rev. B **80**, 024425 (2009).
[15] T. O. Strandberg, C. M. Canali, and A. H. MacDonald, Phys. Rev. B **81**, 054401 (2010).
[16] J.-M. Tang and M. E. Flatté, Phys. Rev. Lett. **92**, 047201 (2004).
[17] J.-M. Tang and M. E. Flatté, Phys. Rev. B **72**, 161315 (2005).
[18] C. M. Canali *et al.*, Phys. Rev. Lett. **91**, 046805 (2003).
[19] T. O. Strandberg *et al.*, Phys. Rev. B **77**, 174416 (2008).
[20] R. Resta, J. Phys.: Condens. Matter **12**, 107 (2000).
[21] Auerbach, Interacting Electron and Quantum Magnetism (Springer-Verlag, New York, 1994).
[22] B. Simon, Phys. Rev. Lett. **51**, 2167 (1983).
[23] Due to tetrahedral symmetry, the energy dependence on the Mn moment for one impurity in bulk GaAs vanishes within approaches not based on finite clusters[17]. In our approach it consistently decreases with cluster size[14]. A 1200-atom cluster is sufficient for capturing the physics of the effective spin and yields the correct value of J.
[24] To treat this case, we consider a GaAs cluster with a (110) surface exposed, and apply periodic boundary conditions in the other two directions. The surface atoms are relaxed as described Ref. 14.